Appl. Phys. B 69, 501–504 (1999) / Digital Object Identifier (DOI) 10.1007/s003409900194

Applied Physics B
Lasers
and Optics

Rapid communication

Reflection of a slow cesium atomic beam from a naturally magnetized Nd-Fe-B surface

F. Lison, D. Haubrich, P. Schuh, D. Meschede

Institut für Angewandte Physik, Universität Bonn, Wegelerstr. 8, 53115 Bonn, Germany
(Fax: +49-228/733474, E-mail: sek@iap.uni-bonn.de)

Received: 5 July 1999/Revised version: 6 October 1999/Published online: 3 November 1999

Abstract. We have demonstrated the partly directed reflection of a slow cesium atomic beam by using the natural magnetic stray field above a Nd-Fe-B surface. From these experiments we determine the reflectivity and a minimum value for the magnetic stray field directly at the surface.

PACS: 03.75.Be; 75.30.Gw; 75.70.Kw

In atom optics, atom-optical analogs of photonic optical components such as lenses, beamsplitters, and mirrors are fabricated [1]. There have been two main approaches in the construction of atomic mirrors: evanescent light waves [2] and spatially varying magnetic fields [3]. The first realization of an atomic mirror utilized an evanescent light wave [4]. During the last few years magnetic mirrors which use the Zeeman interaction between an atomic magnetic moment and an inhomogeneous magnetic field have become more and more popular. Flat atomic mirrors have been constructed using magnetic recording media [5], macroscopic permanent magnets [6, 7] and microfabricated electromagnetic devices [8]. Hughes *et al.* also formed curved magnetic mirrors from magnetic recording media [9, 10]. Recently, the focusing of atoms by using a curved magnetic mirror fabricated from video tape has been demonstrated [11]. Roach et al. also reported the high but not specular reflectivity of demagnetized audio tape [5].

All these magnetic mirrors are based on a periodic magnetization changing direction with a period of λ. This leads to an approximately exponentially decaying magnetic flux density above the magnetic surface [12, 13]. The decay constant is $2\pi/\lambda$ and the maximum surface field limits the normal atomic velocity that can be reflected. The construction of mirrors from magnetic recording media has the advantage of smaller magnetization periods and smoother equipotential planes. The advantage of mirrors fabricated from permanent magnets is that the magnetic field strength is an order of magnitude larger. Moreover the suppression of the magnetic field outside the material due to the finite thickness of the magnetic material is not relevant for bulk material, whereas this reduction is typically 30% for magnetic recording media.

The natural domain structure in ferromagnets which are not externally magnetized could provide a simple way to achieve both a high surface field strength of the order of 1 T and a magnetization period in the micron regime. Mirrors with these properties are needed for magnetic imaging schemes with laser-cooled atomic beams in grazing-incidence geometries.

In the absence of external fields the demagnetized state is the stable state in large ferromagnetic crystals and for this state the free energy is minimal. The resulting domain structure is then a consequence of balancing various contributions to the free energy in order to minimize it [14]. For our purpose the most interesting contribution is the anisotropy energy. It arises from the existence of preferred ("easy") axes of magnetization in ferromagnetic crystals. No domains of closure can form in a specimen with very strong magnetic anisotropy and only one easy axis orientated perpendicular to one of its surfaces exists. Consequently a magnetic field leaks out and forms a stray field immediately above the surface. The internal and surface domains will then self-organize in order to minimize the contribution of the magnetic stray field to the free energy. This results in a domain pattern with alternating magnetization which is in one dimension similar to an atomic mirror built from permanent magnets.

In this paper we describe the surface properties and magnetic stray field of a naturally magnetized Nd-Fe-B surface. We then use this field to reflect a Zeeman-slowed cesium atomic beam.

1 Surface preparation and characterization

A sintered Nd-Fe-B cuboid with dimensions $90 \times 30 \times 10\,\mathrm{mm}^3$ was obtained from Magnetfabrik Schramberg [15]. The cuboid was polished with abrasive paper and a fine finish was accomplished using crystal polish powder. Figure 1a shows a difference interference contrast image of the surface, which was used to obtain a general overview.

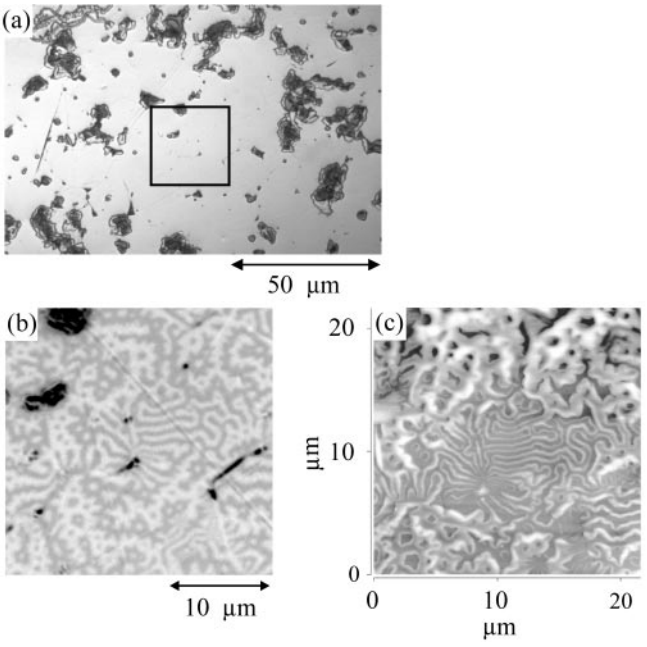

Fig. 1. a Difference interference contrast image of the polished Nd-Fe-B surface. *Bright regions* are flat areas and *dark regions* are grooves. **b** Magnetic domain structure of the squared region in a imaged with a polarizing microscope. The axis of easy magnetization is perpendicular to the surface shown. **c** Same region imaged with a magnetic force microscope. One can clearly see that both techniques show the same domain structure

Approximately 80% of the surface is flat, whereas the remainder contains cavities. Further polishing did not reduce the portion of the surface covered with cavities because sintered Nd-Fe-B is only 97% dense. For a quantitative analysis we inspected the flat parts of the surface by means of atomic force microscopy (SIS Ultra objective). The rms roughness of the surface was determined to be 50 nm on a $20 \times 20\,\mu m^2$ scale and reduces to 7 nm on a $5 \times 5\,\mu m^2$ area. This is to be compared with a rms roughness of 100 nm for the original unpolished surface. Once polished the material has to be kept under vacuum conditions because the effect of corrosion upon Nd-Fe-B magnets is serious.

The sintered Nd-Fe-B material consists primarily of aligned grains of the tetragonal $Fe_{14}Nd_2B$ phase. These grains possess a high magnetic anisotropy with the easy axis being normal to the polished surface. The material also contains non-magnetic secondary grain boundary phases into which excess Nd and B atoms diffuse. Typical values for the grain size are 5–10 μm. Magnetic domains were observed by using a magnetic force and a polarizing microscope at normal incidence on the polished surface. Owing to the Kerr effect, domains with different direction of magnetization appear as dark and bright regions [16]. The spontaneous magnetization M_S of the domains is $M_S = 1.63\,T/\mu_0$ [17]. Figure 1b shows the typical dendritic domain structure of a Nd-Fe-B surface [18]. Domains in the surface grains are subdivided to reduce magnetostatic energy. This is also accomplished by additional small point-like domains inside larger domains, which can be clearly seen in Fig. 1b, c. From these images we determine a mean lateral size of the magnetic domains of approximately 1 μm. A one-dimensional periodic arrangement of the domains would result in a decay of the lowest spatial Fourier component of the stray field with a decay length of roughly 0.2 μm. However, due to the stochastic domain structure it seems feasible that also lower spatial Fourier components exist, leading to a slower decay of the stray field.

2 Experiment

Our beam source (Fig. 2) is a Zeeman-slower which produces a slow and cold cesium atomic beam with a mean longitudinal velocity in the range 35 to 120 m/s, a longitudinal velocity spread of less than 1 m/s, and a current of about 10^{10} atoms/s [19]. The final atomic beam has a diameter of 3 mm and a transverse velocity width below the Doppler limit, which corresponds to 12.5 cm/s for cesium. All the atoms are in the $F = 4$ substate. An optical polarization stage is used to pump all the atoms into the outermost $m_F = +4$ Zeeman state, which has a constant magnetic moment of $1\,\mu_B$. For detection, the fluorescence of atoms traversing a sheet of resonant laser light is imaged onto an intensified CCD camera.

The setup for the reflection experiment is housed in a second vacuum chamber connected to the source chamber. The Nd-Fe-B cuboid is placed on an electrically driven rotation stage (angular resolution better than 0.3 mrad) which is connected to a translation stage. This translation stage allows us to move the whole assembly perpendicular to the atomic beam axis. Two movable apertures were used to align the magnetic surface parallel to the atomic beam axis to better than 1.7 mrad.

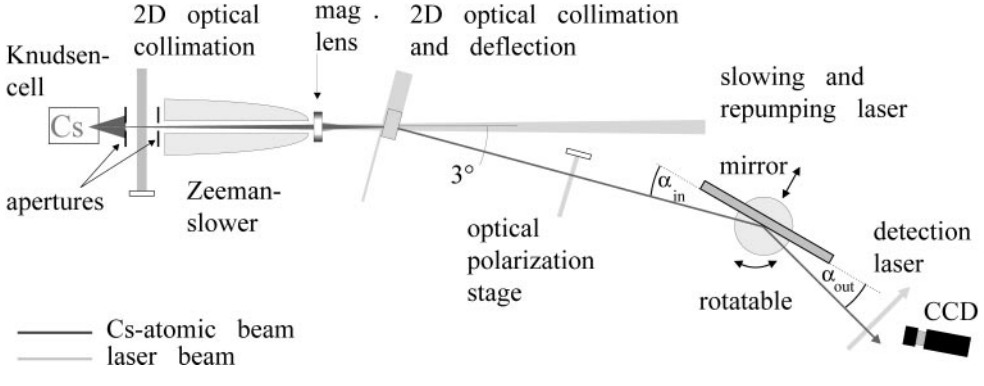

Fig. 2. Experimental setup of the cesium Zeeman-slower and the rotation stage

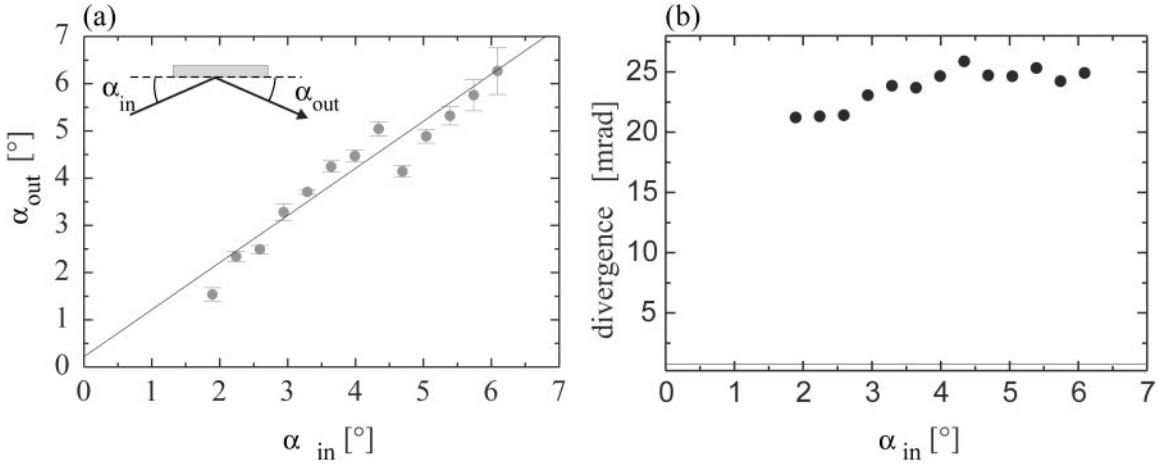

Fig. 3. a Reflection of cesium atoms with a mean longitudinal velocity of 59 m/s. The *error bars* represent only the uncertainty of determining the center of the atomic beam in the CCD images. The *straight line* (slope 1.0, offset 0.2) is the best linear fit to the data points. **b** Divergence of the reflected atomic beam. The *straight line* corresponds to the divergence of the incident atomic beam (0.8 mrad)

Figure 3a shows the mean angle of reflection for grazing angles of incidence of up to 6°. For each data point the deflected atomic beam was alternately monitored at two different positions separated by a distance of 23 mm. We observed the atomic fluorescence with the CCD camera looking perpendicular to the atomic beam axis and the detection laser. From a Gaussian fit to the atomic fluorescence we determined the center and width of the atomic beam at both positions. Using the translation stage we removed the Nd-Fe-B cuboid from the atomic beam axis and monitored the undeflected atomic beam. All these data points were taken without moving the CCD camera. This enables us to calculate the angle of reflection independently from the angle of incidence. Within the experimental uncertainty, the angle of incidence equals the angle of reflection. In Fig. 3b we compare the divergence of the incident atomic beam with the divergence of the reflected atomic beam at different angles of incidence. After the reflection the beam is still well collimated although the divergence has been increased by approximately a factor of 25. From this fact we conclude that at least a part of the atomic beam undergoes directed reflection. We attribute the increase in divergence to the roughness of the magnetic equipotential lines induced by imperfect domain structures and mechanical surface roughness.

In a second series of measurements we observed the atomic fluorescence with the CCD camera looking in the direction of the atomic beam axis. Typical atomic beam profiles for the incident and the reflected atom beam are shown in Fig. 4a. Owing to the larger divergence of the reflected beam the corresponding atomic beam profiles are wider. In Fig. 4b we compare the number of atoms in the reflected and incident atomic beam. For small angles of incidence the overall reflectivity of the Nd-Fe-B surface is as high as 100%. It drops with increasing angle of incidence because more and more atoms are able to reach the surface within regions of lower magnetic potential. Using the known longitudinal velocity and the maximum angle of incidence, we can estimate the surface field to be approximately 0.9 T. This corresponds to a value of $0.55\mu_0 M_S$ and is about 75% of the magnetic

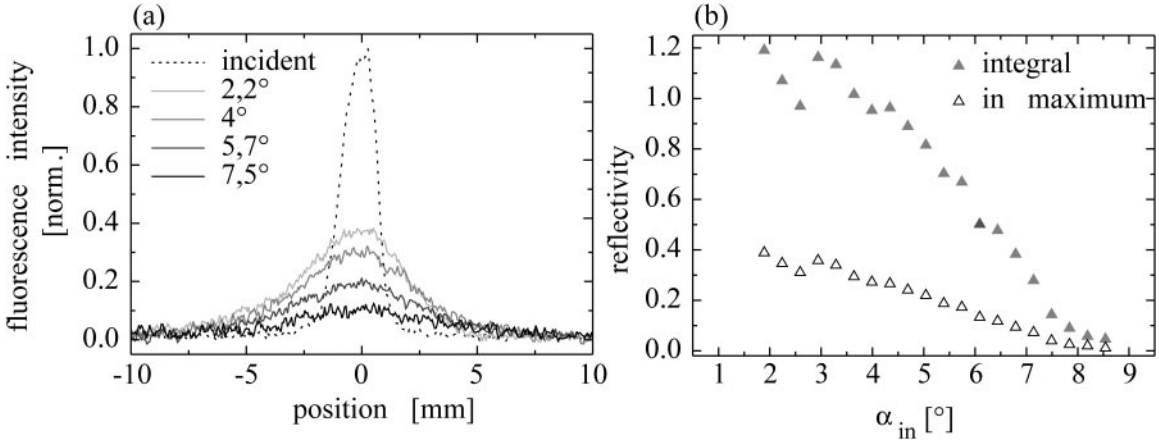

Fig. 4. a Atomic beam profiles of incident (*dashed line*) and reflected atomic beams (*solid lines*) for different angles of incidence. Each profile is an average over 10 lines (0.6 mm) in the CCD image containing the center of the atomic beam. The profiles are taken in the direction perpendicular to the mirror surface. **b** Reflectivity of the Nd-Fe-B surface for different angles of incidence. Values larger than 1 are due to fluctuations in the atomic current and detection efficiency. The *solid symbols* show the number of atoms integrated over the complete atomic beam profile. The *open symbols* compare the peak value of the fluorescence intensity in the corresponding beam profiles

remanence that the fully magnetised Nd-Fe-B cuboid would have. In Fig. 4b we also show the ratio of the peak values for the fluorescence intensity of the reflected and incident atomic beams. This ratio should be unity for fully specular reflection.

We were not able to observe the reflection of slow cesium atoms from the unpolished back surface of the Nd-Fe-B cuboid, although a reflectivity of less than 1% would have been detectable. This confirms that the surface roughness of the specimen is a critical parameter for the atom-optical properties of this magnetic mirror.

3 Conclusion

We have demonstrated a type of magnetic mirror for atoms which makes use of the stray field of ferromagnetic materials. This magnetic mirror is a passive atom-optical element, very robust and easy to fabricate, but the atom-optical properties of this type of magnetic mirror are not yet satisfactory. Nevertheless we have seen partly directed reflection of atoms from its surface. From our reflection data we were able to determine the value of the magnetic stray field immediately above the surface to be about 0.9 T.

The performance of such a mirror could be improved by using a different ferromagnetic specimen. The new material should provide a highly regular domain structure, which is difficult to achieve in the sintered and hence inhomogeneous Nd-Fe-B material. A candidate promising a more regular domain structure with several 10 μm of scaling length would be a sufficiently large single crystal of cobalt [20].

Acknowledgements. F. Lison acknowledges valuable discussions with I.G. Hughes.

References

1. C.S. Adams: Contemp. Phys. **35**, 1 (1994)
2. J.P. Dowling, J. Gea-Banacloche: Adv. At., Mol., Opt. Phys. **37**, 1 (1996)
3. E.A. Hinds, I.G. Hughes: J. Phys. D. **32**, R119 (1999)
4. V.I. Balykin, V.S. Letokhov, Y.B. Ovchinnikov, A.I. Sidorov: JETP Lett. **45**, 353 (1987)
5. T. Roach, H. Abele, M.G. Boshier, H.L. Grossman, K.P. Zetie, E.A. Hinds: Phys. Rev. Lett. **75**, 629 (1995)
6. A.I. Sidorov, R.J. McLean, W.J. Rowlands, D.C. Lau, J.E. Murphy, M. Walkiewicz, G.I. Opat, P. Hannaford: Quantum Semiclass. Opt. **8**, 713 (1996)
7. D. Meschede, I. Bloch, A. Goepfert, D. Haubrich, M. Kreis, F. Lison, R. Schütze, R. Wynands: in *Atom Optics*, ed. by M.G. Prentiss, W.D. Phillips, Procd. SPIE **2995**, 191 (1997)
8. D.C. Lau, A.I. Sidorov, G.I. Opat, R.J. McLean, W.J. Rowlands, P. Hannaford: Eur. Phys. J. D **5**, 193 (1999)
9. I.G. Hughes, P.A. Barton, T.M. Roach, M.G. Boshier, E.A. Hinds: J. Phys. B: At. Mol. Opt. Phy. **30**, 647 (1997)
10. I.G. Hughes, P.A. Barton, T.M. Roach, E.A. Hinds: J. Phys. B: At. Mol. Opt. Phys. **30**, 2119 (1997)
11. C.V. Saba, P.A. Barton, M.G. Boshier, I.G. Hughes, P. Rosenbusch, B.E. Sauer, E.A. Hinds: Phys. Rev. Lett. **82**, 468 (1999)
12. V.V. Vladimirski: Sov. Phys. JETP **12**, 740 (1961)
13. G.I. Opat, S.J. Wark, A. Cimmino: Appl. Phys. B **54**, 396 (1992)
14. C. Kittel: Rev. Mod. Phys. **21**, 541 (1949)
15. Magnetfabrik Schramberg, 1997, Product information about Seltenerdmagnet NdFeB 270/95h (in German)
16. H.J. Williams, F.G. Foster, E.A. Wood: Phys. Rev. **82**, 119 (1951)
17. B. Grieb, PhD thesis, Universität Stuttgart, Germany (1991)
18. J.D. Livingston: J. Appl. Phys. **57**, 4137 (1985)
19. F. Lison, P. Schuh, D. Haubrich, D. Meschede: Phys. Rev. A, **61** (2000)
20. W. Szmaja: J. Magn. Magn. Mater. **153**, 215 (1996)